

Theoretical considerations on the free-surface role in the smoothed-particle-hydrodynamics model

Andrea Colagrossi*

*The Italian Ship Model Basin (INSEAN), Via di Vallerano 139, 00128 Roma, Italy
and Centre of Excellence for Ship and Ocean Structures (CESOS), NTNU, Trondheim, Norway*

Matteo Antuono†

The Italian Ship Model Basin (INSEAN), Via di Vallerano 139, 00128 Roma, Italy

David Le Touzé‡

École Centrale Nantes, Fluid Mechanics Laboratory, CNRS UMR6598, 1 rue de la Noë, 44300 Nantes, France

(Received 7 November 2008; published 6 May 2009)

In the present work, an in-depth analysis of the theoretical structure of the smoothed-particle hydrodynamics (hereinafter SPH) is provided for an inviscid, weakly compressible, and barotropic flow *in the presence of a free surface*. The role of the free surface in the SPH scheme is indeed little addressed in literature. In the present analysis, the general continuous formulation of the SPH method is considered. A detailed description of the free-surface influence on the smoothed differential operators is supplied. New and existing forms are analyzed in detail, in terms of convergence and conservation properties. The proposed analysis is based on the principle of virtual works, which permits to exhibit the link with the enforcement of the dynamic free-surface boundary condition. Finally, possible SPH formulations resulting from this analysis are investigated, in terms of consistency, conservation, and dynamic free-surface boundary condition.

DOI: [10.1103/PhysRevE.79.056701](https://doi.org/10.1103/PhysRevE.79.056701)

PACS number(s): 47.11.-j

I. INTRODUCTION

In the last two decades, a class of numerical solvers based on the use of meshless scattered sets of nodes has started to be successfully applied to various physical problems. In the case of complex problems dominated by advection phenomena and characterized by the presence of deformable interfaces, the discretization methods commonly applied, such as finite-difference, finite-element, or finite-volume methods, can have difficulties and dedicated numerical techniques are required to find effective solutions. Such problems can be effectively solved by particle methods such as the smoothed-particle hydrodynamics (SPH) first proposed in [1,2]. The simplicity and flexibility of the SPH scheme have led to a wider and wider range of applications, spreading from the astrophysics to the fluid dynamics among many other fields. In the specific, in the case of fluid motions characterized by a complex free-surface evolution (e.g., including multiple wave-breaking events), the careful implementation of the SPH has proved to be very robust and fairly accurate (see, e.g., [3]).

Notwithstanding the wider and wider diffusion of the SPH methods, up to today there is no specific theoretical analysis of such a meshless scheme for free-surface flows. Namely, no detailed description has been given of the influence of the terms associated to the free surface. The aim of the present work is, therefore, to address this lack and provide useful considerations for the free-surface SPH practitioners. The

main steps lying under the SPH method formulation are (1) the continuous integral interpolation used to approximate the spatial differential operators and (2) the discretization of such convolution integrals into a finite set of elementary fluid volumes. It should be underlined that the main characteristics, properties, and drawbacks of the SPH are a consequence of the continuous integral interpolation. Point (1) is thus the main object of the present analysis.

In this context, the presence of a free surface has two main consequences: physical boundary conditions have to be satisfied on this surface and the interpolation accuracy has to be preserved close to the domain boundary. Indeed, when achieving the SPH interpolation, some surface terms appear in both the pressure gradient and velocity divergence terms. However, such terms are generally neglected by the SPH practitioners. Their deletion generally leads to pressure gradient formulas which do not converge to the right values near the free surface. Conversely, it is highlighted in the present paper that the continuous divergence operator converges even if the surface terms are not taken into account. For these reasons, an in-depth analysis of their influence and order of convergence is performed in the present work.

Then, the extension of the Bonet and Lok [4] work in the continuous space is defined through the use of the principle of virtual work (hereinafter PVW). The latter, taking into account the balance between the work associated to the fluid volume and the work due to the free-surface motion, allows obtaining a pressure gradient formulation which satisfies the main conservation properties of the fluid. Doing this, we also show how the dynamic free-surface boundary condition is enforced in a weak way, that is, using an integral formulation. Various forms of the smoothed differential operators are analyzed in detail, in terms of convergence and conservation

*a.colagrossi@insean.it

†matteoantuono@gmail.com

‡david.letouze@ec-nantes.fr

properties. Using this methodology, resulting SPH formulations of the governing equations are discussed.

In the present paper, Sec. II introduces the governing equations and the boundary conditions on the rigid boundaries and the free surface. Section III deals with the SPH integral interpolation. The behavior of the convolution integrals close to the free surface is analyzed as the characteristic length of the kernel support goes to zero, and the surface terms are introduced. Then, Sec. IV describes the principle of virtual works which provides a methodology (based on a Lagrangian variational principle) for analyzing the properties of SPH formulations. The link with the enforcement of the dynamic free-surface boundary condition is also exhibited. Finally, in Sec. V SPH formulations resulting from this analysis are investigated, in terms of consistency, conservation, and dynamic free-surface boundary condition. The effectiveness of the most interesting formulation in this respect is illustrated on a practical problem.

II. GOVERNING EQUATIONS

A. Field equations

In physical problems with free-surface, the SPH scheme is generally based on the assumption that the fluid is inviscid and the flow is free to have rotational motion. The problem is thus governed by the Euler equation in the fluid domain Ω which in Lagrangian formalism reads as

$$\frac{D\mathbf{u}}{Dt} = -\frac{\nabla p}{\rho} + \mathbf{f}, \quad (1)$$

where \mathbf{u} is the fluid velocity defined as follows:

$$\frac{D\mathbf{x}}{Dt} = \mathbf{u}, \quad (2)$$

\mathbf{x} is the material point position, \mathbf{f} is a generic external force field, ρ is the fluid density, and p is the pressure field.

Two different strategies can then be adopted to model free-surface flows. The first one is to consider that the liquid is incompressible, implying that its velocity \mathbf{u} is divergence free. Inserting this constraint into the Euler equation leads to a Poisson equation for the pressure field p . The second strategy (usually adopted in free-surface SPH) considers the flow as compressible. Therefore, an equation of state $p=p(\rho, e)$ is required, where e is the specific internal energy. Together with the Euler equation, the continuity equation

$$\frac{D\rho}{Dt} = -\rho \operatorname{div} \mathbf{u} \quad (3)$$

and the internal energy equation

$$\rho \frac{De}{Dt} = -p \operatorname{div} \mathbf{u} \quad (4)$$

have to be considered. In the latter form (4) of the internal energy equation, no entropy source terms are considered, so the fluid is barotropic, which means that pressure p and internal energy e are both single-valued functions of density ρ . It implies also that the latter Eq. (4) is decoupled from the other governing Eqs. (1) and (3).

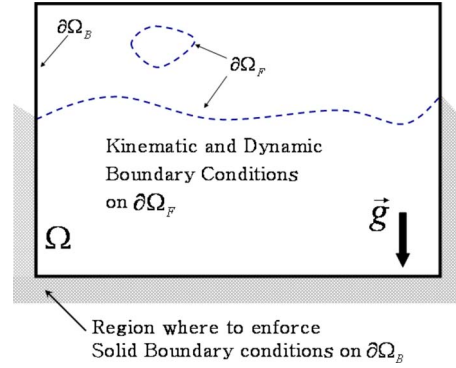


FIG. 1. (Color online) Sketch of the fluid domain with solid boundaries and a free surface.

B. Boundary conditions

The fluid boundary $\partial\Omega$ is composed by a free surface $\partial\Omega_F$ and by solid boundaries $\partial\Omega_B$. On solid boundaries $\partial\Omega_B$, a free-slip condition is assumed

$$\mathbf{u} \cdot \mathbf{n}_B = \mathbf{V}_{\partial\Omega_B} \cdot \mathbf{n}_B \quad \forall \mathbf{x} \in \partial\Omega_B, \quad (5)$$

where \mathbf{n}_B is a vector normal to the boundary $\partial\Omega_B$ and $\mathbf{V}_{\partial\Omega_B}$ is the boundary velocity. A way to enforce this condition is to use a local mirroring of the flow on the other side of the solid boundary (see, e.g., [5]). Figure 1 gives an idea of such a mirroring procedure.

On the free surface, two conditions must be verified. The kinematic condition (hereinafter KFSBC) implies that the fluid particles initially on $\partial\Omega_F$ will remain on the boundary; it writes

$$\mathbf{u} \cdot \mathbf{n}_F = \mathbf{V}_{\partial\Omega_F} \cdot \mathbf{n}_F \quad \forall \mathbf{x} \in \partial\Omega_F, \quad (6)$$

where \mathbf{n}_F is a vector normal to $\partial\Omega_F$ and $\mathbf{V}_{\partial\Omega_F}$ is the boundary velocity. This condition is implicitly verified since a Lagrangian formalism is used in SPH (after discretization, such a condition is only approximately satisfied).

As no surface tension is taken into account, the dynamic condition along the free surface (hereinafter DFSBC) states that the pressure is continuous across $\partial\Omega_F$, therefore equal to the external pressure p_e

$$p = p_e \quad \forall \mathbf{x} \in \partial\Omega_F. \quad (7)$$

When p_e is constant, a trivial change in the pressure reference leads to $p=0$ on the free surface, which is commonly used by SPH practitioners. It must be noted that since the pressure is constant on the free surface, the density has—also—to be constant there (barotropic flow). As a consequence, the continuity (3) reads as

$$\operatorname{div} \mathbf{u} = 0 \quad \forall \mathbf{x} \in \partial\Omega_F. \quad (8)$$

The verification of the dynamic free-surface condition is however a difficult point of the SPH method, rarely deeply discussed in literature. Section III addresses in detail this point.

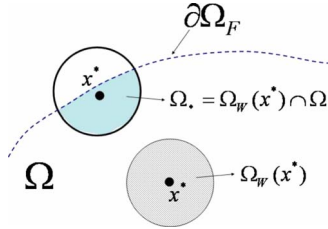


FIG. 2. (Color online) Sketch of the interpolation support.

III. SPH INTEGRAL INTERPOLATION

A. Interpolation of functions and their gradients

In meshless methods, the field of a generic quantity f is interpolated through a convolution integral over the domain Ω ,

$$\langle f \rangle(\mathbf{x}) = \int_{\Omega} f(\mathbf{x}^*) W(\mathbf{x} - \mathbf{x}^*; h) dV^*, \quad (9)$$

in which $W(\mathbf{x} - \mathbf{x}^*; h)$ is a weight function and h is a characteristic length of its bounded support $\Omega_W(\mathbf{x}^*)$ (see Fig. 2). The latter is defined as the area where W differs from zero. Physically, h is also representative of the domain of influence $\Omega_W(\mathbf{x}^*)$ of \mathbf{x}^* . Hereinafter, we denote $W(\mathbf{x} - \mathbf{x}^*; h)$ through $W(\mathbf{x} - \mathbf{x}^*)$ and the dependence on h is understood. The weight function $W(\mathbf{x} - \mathbf{x}^*)$ called *smoothing function* or *kernel* in the SPH framework is positive, radial centered in \mathbf{x}^* , and decreases monotonously with $\|\mathbf{x} - \mathbf{x}^*\|$ to reach zero at the border of its support $\Omega_W(\mathbf{x}^*)$. Finally, we also assume the kernel to be symmetric, that is, $W(\mathbf{x} - \mathbf{x}^*) = W(\mathbf{x}^* - \mathbf{x})$. Its integral

$$\Gamma(\mathbf{x}) = \int_{\Omega_W(\mathbf{x}^*) \cap \Omega} W(\mathbf{x} - \mathbf{x}^*) dV^* \quad (10)$$

is unity inside the domain, i.e., where $\Omega_W(\mathbf{x}^*) \cap \Omega = \Omega_W(\mathbf{x}^*)$. In the following, $\Omega_W(\mathbf{x}^*) \cap \Omega$ is noted Ω_* . When taking the limit as $h \rightarrow 0$, the kernel function W becomes a Dirac delta function, and thus $\langle f \rangle$ turns to be exactly f . As highlighted in [6], the error made in approximating f by its smoothed estimate $\langle f \rangle$ in continuous space (i.e., before applying spatial discretization) is

$$\langle f \rangle = f + O(h^2) \quad \text{where} \quad \Omega_* = \Omega_W(\mathbf{x}^*). \quad (11)$$

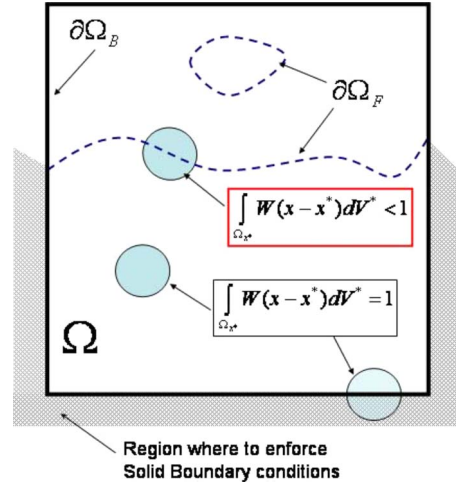
However, after discretization the convergence obtained does not remain as favorable (cf. [7]). Moreover, it must be noted that the relation (11) is not true if $\mathbf{x} \in \partial\Omega_F$, i.e., where $\Omega_* \neq \Omega_W(\mathbf{x}^*)$. In this case it becomes

$$\langle f \rangle = f \lim_{h \rightarrow 0} \Gamma + O(h) \quad (12)$$

and $\lim_{h \rightarrow 0} \Gamma < 1$ (see, for example, Fig. 3). In the specific, if $\partial\Omega_F$ is a regular curve, $\Gamma \rightarrow 1/2$ as h goes to zero and Eq. (12) becomes

$$\langle f \rangle = f/2 + O(h). \quad (13)$$

However, the convergence is recovered if the field f is zero along the free surface. For details, we address the reader to Appendix A.


 FIG. 3. (Color online) Behavior of $\Gamma(\mathbf{x})$ inside the fluid domain and near the boundaries.

The same interpolation can be applied to the gradient of a generic function

$$\langle \nabla f \rangle(\mathbf{x}) = \int_{\Omega_*} \nabla^* f(\mathbf{x}^*) W(\mathbf{x} - \mathbf{x}^*) dV^*, \quad (14)$$

where ∇^* means that the derivatives are computed on the \mathbf{x}^* variable. Integrating by parts, it comes

$$\begin{aligned} \langle \nabla f \rangle(\mathbf{x}) &= \int_{\Omega_*} f(\mathbf{x}^*) \nabla W(\mathbf{x} - \mathbf{x}^*) dV^* \\ &+ \int_{\partial\Omega_*} f(\mathbf{x}^*) W(\mathbf{x} - \mathbf{x}^*) \mathbf{n}^* dS^*, \end{aligned} \quad (15)$$

where \mathbf{n}^* is a vector normal to $\partial\Omega_*$ pointing outside Ω_* and ∇ indicates the derivatives with respect to the variable \mathbf{x} . In the latter equation, the symmetry property of the kernel $\nabla^* W(\mathbf{x} - \mathbf{x}^*) = -\nabla W(\mathbf{x} - \mathbf{x}^*)$ has been used. Through this integration by parts, the gradient of a generic function is accessible from the knowledge of the function itself, which is the key point of meshless methods.

B. Surface integrals

To further analyze the convergence of the smoothed gradient, we consider the following identity:

$$\nabla \Gamma \equiv \int_{\Omega_*} \nabla W(\mathbf{x} - \mathbf{x}^*) dV^* = - \int_{\partial\Omega_*} W(\mathbf{x} - \mathbf{x}^*) \mathbf{n}^* dS^*. \quad (16)$$

Inside the fluid domain, the contour integral is null since W is identically zero along $\partial\Omega_*$ and, therefore, $\nabla \Gamma = 0$ as well. Conversely, near the free surface the contour integral is different from zero and, consequently, $\nabla \Gamma \neq 0$. For the same reasons, inside the fluid domain the last integral of Eq. (15) is identically zero and it becomes

$$\langle \nabla f \rangle(\mathbf{x}) = \int_{\Omega_\star} f(\mathbf{x}^\star) \nabla W(\mathbf{x} - \mathbf{x}^\star) dV^\star. \quad (17)$$

Such a formula is often used in the SPH solvers to approximate the gradient of functions. However, it provides just a rough approximation since it does not converge to the right value near the free surface. This can be easily checked on the following simple example. If f is a constant field (that is, $f \equiv f_0$), $\langle \nabla f \rangle(\mathbf{x}) = 0$ from Eq. (14). Conversely, using Eq. (17), one gets

$$\langle \nabla f \rangle(\mathbf{x}) = f_0 \nabla \Gamma, \quad (18)$$

which does not converge to zero near the free surface (unless $f_0 = 0$). This is a consequence of the fact that the contour integral of Eq. (15) is not zero near the free surface and, therefore, cannot be neglected. This highlights that the evaluation of the smoothed fields near the free surface needs a proper and accurate analysis.

The role of the surface integrals is almost never commented in the free-surface SPH literature. Actually, the surface integral is simply neglected in practice mainly because it is difficult to evaluate. This omission leads afterward free-surface SPH practitioners to use intuitive or empirical modifications of the discrete scheme. To give a rigorous justification to these effective modifications, we keep these surface terms in the present work.

C. Considerations on $\langle \nabla p \rangle$ and $\langle \text{div } \mathbf{u} \rangle$ in the presence of a free surface

In the governing equations, the spatial differential operators needed to march in time are the pressure gradient and the divergence of the velocity field. The SPH scheme is built on the assumption that these operators can be approximated by their smoothed versions. Then, we write

$$\begin{cases} \frac{D\rho}{Dt} = -\rho \text{div}(\mathbf{u}) \\ \frac{D\mathbf{u}}{Dt} = -\frac{\nabla p}{\rho} + \mathbf{f} \end{cases} \Rightarrow \begin{cases} \frac{D\rho}{Dt} = -\rho \langle \text{div } \mathbf{u} \rangle \\ \frac{D\mathbf{u}}{Dt} = -\frac{\langle \nabla p \rangle}{\rho} + \mathbf{f}. \end{cases} \quad (19)$$

If the smoothed operators converge to the exact values for h going to zero then the second system converges to the first one and the SPH scheme is consistent.

For gravity flows, the pressure field is generally almost linear close to the free surface. In such conditions, the interpolation (14) of ∇p close to the free surface is a rough approximation, as previously discussed in Sec. II A, and does not converge to the expected value as h goes to zero. Indeed, let us assume p to be exactly a linear field. As a consequence, we get $\nabla p = C_0$ (where C_0 is a constant different from zero). Substituting it inside Eq. (14), we obtain

$$\langle \nabla p \rangle = C_0 \Gamma. \quad (20)$$

It thus does not converge to the exact value near the free surface (it gives half of the theoretical value on a flat free surface). Since Eq. (14) converges to a wrong value, Eqs. (15) and (17) will do the same.

The divergence of the velocity field is exactly zero along the free surface because of the DFSBC (8). Then, the inter-

polation (14) of $\text{div } \mathbf{u}$ converges to the exact value as h goes to zero. After applying the integration by parts, it comes

$$\begin{aligned} \langle \text{div } \mathbf{u} \rangle(\mathbf{x}) &= \int_{\Omega_\star} \mathbf{u}(\mathbf{x}^\star) \cdot \nabla W(\mathbf{x} - \mathbf{x}^\star) dV^\star \\ &+ \int_{\partial\Omega_\star} \mathbf{u}(\mathbf{x}^\star) \cdot \mathbf{n}^\star W(\mathbf{x} - \mathbf{x}^\star) dS^\star. \end{aligned} \quad (21)$$

In the latter equation, the surface term generally has the same order of magnitude of the volume term and, therefore, it is not possible to neglect it. Indeed, despite Eq. (21) converges, the surface and volume integral are both divergent as $O(1/h)$ (this statement can be easily checked if one computes the divergence by using the Gaussian kernel defined in Appendix B and $\mathbf{u} = \mathbf{u}_0 = \text{const}$). A way to impose the $O(h)$ convergence of both the integral terms of Eq. (21) is to subtract the following identity:

$$\mathbf{u}(\mathbf{x}) \cdot \left[\int_{\Omega_\star} \nabla W(\mathbf{x} - \mathbf{x}^\star) dV^\star + \int_{\partial\Omega_\star} W(\mathbf{x} - \mathbf{x}^\star) \mathbf{n}^\star dS^\star = 0 \right], \quad (22)$$

obtaining

$$\begin{aligned} \langle \text{div } \mathbf{u} \rangle(\mathbf{x}) &= \int_{\Omega_\star} [\mathbf{u}(\mathbf{x}^\star) - \mathbf{u}(\mathbf{x})] \cdot \nabla W(\mathbf{x} - \mathbf{x}^\star) dV^\star \\ &+ \int_{\partial\Omega_\star} [\mathbf{u}(\mathbf{x}^\star) - \mathbf{u}(\mathbf{x})] \cdot \mathbf{n}^\star W(\mathbf{x} - \mathbf{x}^\star) dS^\star. \end{aligned} \quad (23)$$

This behavior allows to neglect the surface integral without affecting the convergence of the divergence operator (see Appendix A). However, the deletion of the surface integral affects the accuracy of the smoothed divergence operator (see Appendix B).

The reason why the SPH practitioners do not consider the surface terms is the great difficulty in the evaluation of the surface integral. This is due to both geometrical problems (complex contour paths) and accuracy issues.

This analysis of the smoothed version of the differential operators close to the free surface shows that the velocity divergence (23) leads to a consistent approximation of the continuity equation. Moreover, this result still holds if the surface term is neglected. Conversely, the pressure gradient approximation is not consistent on the free surface since no convergence is obtained when using formula (15). This will be further addressed in Sec. IV F.

IV. ENFORCEMENT OF THE DFSBC AND LINK WITH THE SPH CONSERVATION PROPERTIES THROUGH THE PRINCIPLE OF VIRTUAL WORK

In the present section, we develop considerations regarding the conservation properties (energy and momenta) of the fluid. This can be done following a Lagrangian variational principle as done by several authors (see, e.g., [8,9]) or equivalently following the variational principle used by Bo-

net and Lok [4]. However, here we rewrite the PVW including the external work part and in *continuous space* rather than after the discretization of the fluid domain into a finite set of particles. Using such a formulation, it is possible to discuss about:

(i) the way in which the DFSBC is enforced in the SPH formulation,

(ii) how it is possible to choose a formulation for ∇p starting on the specific form used for $\text{div } \mathbf{u}$, and

(iii) the role of the mechanical work associated to the surface terms in Eq. (23).

A. PVW

The PVW expresses the equality between the work of the internal forces δW_I and the one of the external forces δW_E due to the virtual displacement field $\delta \mathbf{w}$. It reads in its general form (see, e.g., [10,11]) as

$$\underbrace{\int_{\partial\Omega} \mathbf{T}\mathbf{n} \cdot \delta \mathbf{w} dS}_{\delta W_E} - \underbrace{\int_{\Omega} \rho \mathbf{F} \cdot \delta \mathbf{w} dV}_{\delta W_I} = \int_{\Omega} \mathbf{T} : \mathbf{E}(\delta \mathbf{w}) dV, \quad (24)$$

where \mathbf{T} is the stress tensor, $\rho \mathbf{F}$ are the volume forces (including the inertial one), and $\mathbf{E}(\delta \mathbf{w}) = [\nabla(\delta \mathbf{w}) + \nabla^T(\delta \mathbf{w})]/2$. Under the assumptions made in Sec. I, the PVW reads as

$$\underbrace{\int_{\partial\Omega} (-p)\mathbf{n} \cdot \delta \mathbf{w} dS}_{\textcircled{1}} - \underbrace{\int_{\Omega} (-\nabla p) \cdot \delta \mathbf{w} dV}_{\textcircled{2}} = \underbrace{\int_{\Omega} -p \text{div}(\delta \mathbf{w}) dV}_{\textcircled{3}}. \quad (25)$$

Even though the latter expression is a simple application of the divergence theorem, it expresses the PVW which has an important physical meaning. Indeed, the first two terms [① and ②] represent the work of the stress tensor, respectively, on the free surface and in the fluid domain. Their difference produces a variation in the internal energy ③ [see Eq. (4)] due to the virtual displacement field. The balance of the three integral terms guarantees the conservation of both the linear and angular momenta [4].

B. Enforcement of the DFSBC

For the present PVW analysis, we are not interested in the work due to the motion of solid boundaries, which is considered equal to zero (nonmoving boundaries). Since $p=0$ along $\partial\Omega_F$, the expression (25) becomes

$$-\int_{\Omega} (-\nabla p) \cdot \delta \mathbf{w} dV = \int_{\Omega} -p \text{div}(\delta \mathbf{w}) dV. \quad (26)$$

Such a formula states that the work of the stress tensor inside the fluid domain must be equal to the variation in the internal energy, while the work of the stress tensor along the surface is zero.

Thus, to satisfy the DFSBC in a weak sense within the SPH scheme, it is sufficient to verify the equality (26) using the smoothed operators instead of the ordinary ones. In that

case, no other specific condition has to be explicitly enforced onto that surface. This favorable feature is commonly used by free-surface SPH practitioners. However, it must be underlined that this does not imply the consistency of the smoothed operators chosen for the pressure gradient and the velocity divergence, as it is detailed in the following.

C. PVW for smoothed differential operators

We can now substitute in the PVW form (26) the consistent smoothed operator obtained for the velocity divergence (23). After some algebra (see Appendix C) and under the only assumption of null pressure along $\partial\Omega_F$, it comes that the PVW then reads as

$$\int_{\partial\Omega_F} (-\langle p \rangle) \mathbf{n} \cdot \delta \mathbf{w} dS - \int_{\Omega} (-\langle \nabla p \rangle) \cdot \delta \mathbf{w} dV = \int_{\Omega} -p \langle \text{div}(\delta \mathbf{w}) \rangle dV. \quad (27)$$

To satisfy the DFSBC in a weak way, the surface term should be null and Eq. (27) should become

$$-\int_{\Omega} (-\langle \nabla p \rangle) \cdot \delta \mathbf{w} dV = \int_{\Omega} -p \langle \text{div}(\delta \mathbf{w}) \rangle dV. \quad (28)$$

In Sec. IV D, we propose a different formulation for the smoothed operators which satisfy Eq. (28).

D. Derivation of a conservative form of $\langle \nabla p \rangle$

Since $\langle p \rangle \neq 0$ on $\partial\Omega_F$ for $h > 0$, the expression (27) contains a surface integral which is small but sensibly different from zero. This means that the use of $\langle \text{div } \mathbf{u} \rangle$ and $\langle \nabla p \rangle$ as smoothed differential operators leads to the generation of spurious energy associated to the surface integral of $\langle p \rangle$. In order to avoid such a phenomenon, a different formulation for $\langle \text{div } \mathbf{u} \rangle$ and $\langle \nabla p \rangle$ can be obtained such that the surface integral contribution is identically null for $h > 0$. Actually, since the surface integral $\langle p \rangle$ in Eq. (27) derives from the surface integral of $\langle \text{div } \mathbf{u} \rangle$ (see Appendix C), an effective way is to neglect the latter, that is, to use

$$\langle \text{div } \mathbf{u} \rangle^B(\mathbf{x}) = \int_{\Omega_*} [\mathbf{u}(\mathbf{x}^*) - \mathbf{u}(\mathbf{x})] \cdot \nabla W(\mathbf{x} - \mathbf{x}^*) dV^* \quad (29)$$

instead of Eq. (23). If one then substitutes this expression inside Eq. (26), it comes

$$-\int_{\Omega} (-\langle \nabla p \rangle^B) \cdot \delta \mathbf{w} dV = \int_{\Omega} -p \langle \text{div}(\delta \mathbf{w}) \rangle^B dV, \quad (30)$$

where

$$\begin{aligned} \langle \nabla p \rangle^B(\mathbf{x}) &= \int_{\Omega_*} p(\mathbf{x}^*) \nabla W(\mathbf{x} - \mathbf{x}^*) dV^* \\ &+ p(\mathbf{x}) \int_{\Omega_*} \nabla W(\mathbf{x} - \mathbf{x}^*) dV^*, \end{aligned} \quad (31)$$

which is the continuous version of the pressure gradient for-

mulation proposed by Bonet and Lok [4] using the PVW after discretization. One can note that no surface integral appears in Eq. (30).

It is simple to show that $\langle \nabla p \rangle^B$ behaves as $\langle \nabla p \rangle$ for h going to zero. Indeed, if $\mathbf{x} \notin \partial\Omega_F$, there exists a value of h such that $\Omega_W(\mathbf{x}^*) \subset \Omega$ and, therefore

$$\int_{\Omega_*} \nabla W(\mathbf{x} - \mathbf{x}^*) dV^* = 0 \quad (32)$$

and the second term of the right-hand side of Eq. (31) is zero. Finally, if $\mathbf{x} \in \partial\Omega_F$, $p(\mathbf{x})=0$ and, again, the second term of the right-hand side of Eq. (31) is identically zero. As a consequence, we still have

$$\langle \nabla p \rangle^B = \nabla p \lim_{h \rightarrow 0} \Gamma + O(h). \quad (33)$$

Examples of the convergence for both $\langle \nabla p \rangle$ and $\langle \nabla p \rangle^B$ are shown in Appendix B. In particular, it is shown in Fig. 6 that even though the two approximations exhibit the same behavior when h goes to zero, the mean error of $\langle \nabla p \rangle^B$ close to the free surface is lower than the one of $\langle \nabla p \rangle$.

E. Recovering the pressure gradient convergence: The Shepard kernel

As shown in Secs. IV A–IV D, both $\langle \nabla p \rangle^B$ and $\langle \nabla p \rangle$ do not converge to the exact value for h going to zero if $\mathbf{x} \in \partial\Omega_F$. As a consequence, large errors are generally generated for $h > 0$ in a region near to the free surface. In order to avoid such an unfavorable behavior, a renormalization of the kernel can be used. Actually, from Eq. (12) we know that

$$\langle \nabla p \rangle = \nabla p \lim_{h \rightarrow 0} \Gamma + O(h). \quad (34)$$

Then, the most natural renormalization of the kernel is

$$W^S(\mathbf{x} - \mathbf{x}^*) = \frac{W(\mathbf{x} - \mathbf{x}^*)}{\Gamma(\mathbf{x})}, \quad (35)$$

which is the so-called ‘‘Shepard kernel’’ [12]. Using such a kernel, we get the Shepard pressure gradient

$$\langle \nabla p \rangle^S(\mathbf{x}) = \frac{1}{\Gamma(\mathbf{x})} \int_{\Omega_*} \nabla p(\mathbf{x}^*) W(\mathbf{x} - \mathbf{x}^*) dV^*. \quad (36)$$

Integrating by parts and assuming $p=0$ at the free surface, we obtain

$$\langle \nabla p \rangle^S(\mathbf{x}) = \frac{1}{\Gamma(\mathbf{x})} \int_{\Omega_*} p(\mathbf{x}^*) \nabla W(\mathbf{x} - \mathbf{x}^*) dV^*. \quad (37)$$

Finally, we can also define

$$\langle \text{div } \mathbf{u} \rangle^S(\mathbf{x}) = \frac{\langle \text{div } \mathbf{u} \rangle(\mathbf{x})}{\Gamma(\mathbf{x})}. \quad (38)$$

The Shepard pressure gradient converges to the exact value for h going to zero all over the fluid domain and, therefore, it should be preferred to $\langle \nabla p \rangle$ and $\langle \nabla p \rangle^B$. However, if one uses Eq. (37) together with either $\langle \text{div } \mathbf{u} \rangle$ or $\langle \text{div } \mathbf{u} \rangle^B$, the PVW (28) is no more verified, thus leading to the generation of

spurious energy due to the presence of the free surface. As a consequence, the linear and angular momenta will also not be preserved for $h > 0$ (that is, for h sensibly different from zero).

F. Symmetrized Shepard kernel

In order to recover the verification of the PVW (28) using the Shepard kernel, we propose to use the following symmetrized form for the pressure gradient:

$$\langle \nabla p \rangle^C(\mathbf{x}) = \int_{\Omega_*} \left[\frac{p(\mathbf{x}^*)}{\Gamma(\mathbf{x})} + \frac{p(\mathbf{x})}{\Gamma(\mathbf{x}^*)} \right] \nabla W dV^*. \quad (39)$$

Thanks to its symmetricity, such a formula preserves both the linear and angular momenta for h sensibly different from zero and converges to the exact pressure gradient for $h \rightarrow 0$.

Note that it is possible to write

$$\langle \nabla p \rangle^C(\mathbf{x}) = \langle \nabla p \rangle^S(\mathbf{x}) + p(\mathbf{x}) \int_{\Omega_*} \frac{\nabla W}{\Gamma(\mathbf{x}^*)} dV^*. \quad (40)$$

Then, since $\langle \nabla p \rangle^S$ is convergent everywhere, we just need to prove that

$$\lim_{h \rightarrow 0} p(\mathbf{x}) \int_{\Omega_*} \frac{\nabla W}{\Gamma(\mathbf{x}^*)} dV^* = 0 \quad (41)$$

everywhere. If $\mathbf{x} \in \partial\Omega_F$, then $p(\mathbf{x})=0$ and the previous limit holds true. If $\mathbf{x} \notin \partial\Omega_F$, it is always possible to choose a value of h such that $\Gamma(\mathbf{x}^*)=1$. As a consequence, it is possible to write

$$\lim_{h \rightarrow 0} p(\mathbf{x}) \int_{\Omega_*} \frac{\nabla W}{\Gamma(\mathbf{x}^*)} dV^* = \lim_{h \rightarrow 0} p(\mathbf{x}) \int_{\Omega_*} \nabla W dV^* = 0 \quad (42)$$

and the last limit holds true because of the properties of $\nabla \Gamma(\mathbf{x})$.

Using the PVW, it is possible to associate another divergence formula to $\langle \nabla p \rangle^C$ still following the same procedure as in Appendix C:

$$\langle \text{div } \mathbf{u} \rangle^C(\mathbf{x}) = \int_{\Omega_*} [\mathbf{u}(\mathbf{x}^*) - \mathbf{u}(\mathbf{x})] \cdot \frac{\nabla W}{\Gamma(\mathbf{x}^*)} dV^*. \quad (43)$$

Unfortunately, such a formula does not converge to the exact value at the free surface and, therefore, it will be not considered in the following.

One can note that another possible couple of renormalized smoothed operators, which do satisfy the PVW, are

$$\langle \text{div } \mathbf{u} \rangle^D(\mathbf{x}) = \int_{\Omega_*} [\mathbf{u}(\mathbf{x}^*) - \mathbf{u}(\mathbf{x})] \cdot \frac{\nabla W}{\Gamma(\mathbf{x})} dV^*,$$

$$\langle \nabla p \rangle^D(\mathbf{x}) = \int_{\Omega_*} \left[\frac{p(\mathbf{x}^*)}{\Gamma(\mathbf{x}^*)} + \frac{p(\mathbf{x})}{\Gamma(\mathbf{x})} \right] \nabla W dV^*, \quad (44)$$

whose properties are reported in Sec. V.

TABLE I. Consistency of the smoothed operators close to the free surface.

$\text{div}(\mathbf{u})$	$O(h)$	∇p	$O(h)$
$\langle \text{div } \mathbf{u} \rangle$	Yes	$\langle \nabla p \rangle$	No
$\langle \text{div } \mathbf{u} \rangle^B$	Yes	$\langle \nabla p \rangle^B$	No
$\langle \text{div } \mathbf{u} \rangle^C$	No	$\langle \nabla p \rangle^C$	Yes
$\langle \text{div } \mathbf{u} \rangle^D$	Yes	$\langle \nabla p \rangle^D$	No
$\langle \text{div } \mathbf{u} \rangle^S$	Yes	$\langle \nabla p \rangle^S$	Yes

V. SPH FORMULATION OF THE GOVERNING EQUATIONS

In a practical SPH implementation of the governing Eq. (19), one needs two smoothed differential operators to march the equations in time, the pressure gradient, and the velocity divergence. In Secs. IV A–IV F, a number of variants of these smoothed operators have been presented and analyzed. They are summarized in Table I with the associated convergence property.

Different combinations of these operators lead to different SPH formulations. A number of these combinations are analyzed in Table II. Combinations excluded are both nonconvergent operators and nonconvergent velocity divergence together with a nonconservative pressure gradient. Moreover, since the smoothed operators $\langle \text{div } \mathbf{u} \rangle$ and $\langle \text{div } \mathbf{u} \rangle^S$ involve the evaluation of surface terms which are very difficult to calculate numerically, we considered only their combination with $\langle \nabla p \rangle$ and $\langle \nabla p \rangle^S$, respectively, even though they are hardly usable in practice. Finally, as $\langle \text{div } \mathbf{u} \rangle^D$ is similar to $\langle \text{div } \mathbf{u} \rangle^B$ but less accurate, we also only considered its combination with $\langle \nabla p \rangle^D$.

In Table II, the formulations are subdivided into two groups: nonconservative formulations in the upper part and conservative ones in the lower part. Only the conservative ones should be retained for practical implementation. Among these, the last two are the most interesting; the first one (B, B) is classically used in SPH whereas the second one is new and has the specificity of being consistent, although not verifying the PVW. The couple (B, C) is thus the only one which is both consistent and conservative. All these formulations and their properties need to be further evaluated after

discretization which will be achieved in a second paper. Figure 4 shows an example of a simulation obtained using the numerical scheme proposed in [3] with the couple (B, C), proving that such a formulation can be effectively implemented into an SPH solver. Note that the numerical scheme differs from the theoretical one just for the use of the artificial viscosity [9]. Such a term does not represent a physical viscosity and is generally used to stabilize the SPH solvers. The illustrative application is a highly nonlinear sloshing problem. The total loads on the tank walls and the free-surface evolution show a good agreement with the outputs from a boundary element method (BEM) simulation [13]. Note that the comparison is not possible for all the time instants since the BEM code stops when the wave breaks.

VI. CONCLUSIONS

An in-depth inspection of the theoretical properties of the SPH at the continuous level has been provided for an inviscid, weakly compressible, and barotropic flow *with a free surface*. Such an analysis allows to give a theoretical foundation to some of the SPH practitioners approximations and to propose a methodology to derive other approximations. A detailed description of the free-surface influence on the smoothed differential operators has been supplied. The main formulations for both the divergence of the velocity and the pressure gradient have been analyzed in detail, in terms of convergence and conservation properties. New forms of these operators have also been proposed and studied. The proposed analysis is based on the application of the principle of virtual works, which also permits to exhibit the link with the enforcement of the dynamic free-surface boundary condition. A number of SPH formulations resulting from this analysis has been investigated, in terms of consistency, conservation, and dynamic free-surface boundary condition. The most interesting formulations in this respect have been individuated. Among these, the effectiveness of a new one has been illustrated on a practical problem.

ACKNOWLEDGMENTS

This work was partially supported by the Centre for Ships and Ocean Structures (CeSOS), NTNU, Trondheim, within the “Violent Water-Vessel Interactions and Related Structural

TABLE II. Main properties of the different formulations.

$\text{div}(\mathbf{u})$	∇p	Consistency	PVW satisfy ($h > 0$)	Momenta conservation	No need for implementing surface terms
$\langle \text{div } \mathbf{u} \rangle$	$\langle \nabla p \rangle$	No	No	No	No
$\langle \text{div } \mathbf{u} \rangle^S$	$\langle \nabla p \rangle^S$	Yes	No	No	No
$\langle \text{div } \mathbf{u} \rangle^B$	$\langle \nabla p \rangle$	No	No	No	Yes
$\langle \text{div } \mathbf{u} \rangle^B$	$\langle \nabla p \rangle^S$	Yes	No	No	Yes
$\langle \text{div } \mathbf{u} \rangle^B$	$\langle \nabla p \rangle^D$	No	No	Yes	Yes
$\langle \text{div } \mathbf{u} \rangle^C$	$\langle \nabla p \rangle^C$	No	Yes	Yes	Yes
$\langle \text{div } \mathbf{u} \rangle^D$	$\langle \nabla p \rangle^D$	No	Yes	Yes	Yes
$\langle \text{div } \mathbf{u} \rangle^B$	$\langle \nabla p \rangle^B$	No	Yes	Yes	Yes
$\langle \text{div } \mathbf{u} \rangle^B$	$\langle \nabla p \rangle^C$	Yes	No	Yes	Yes

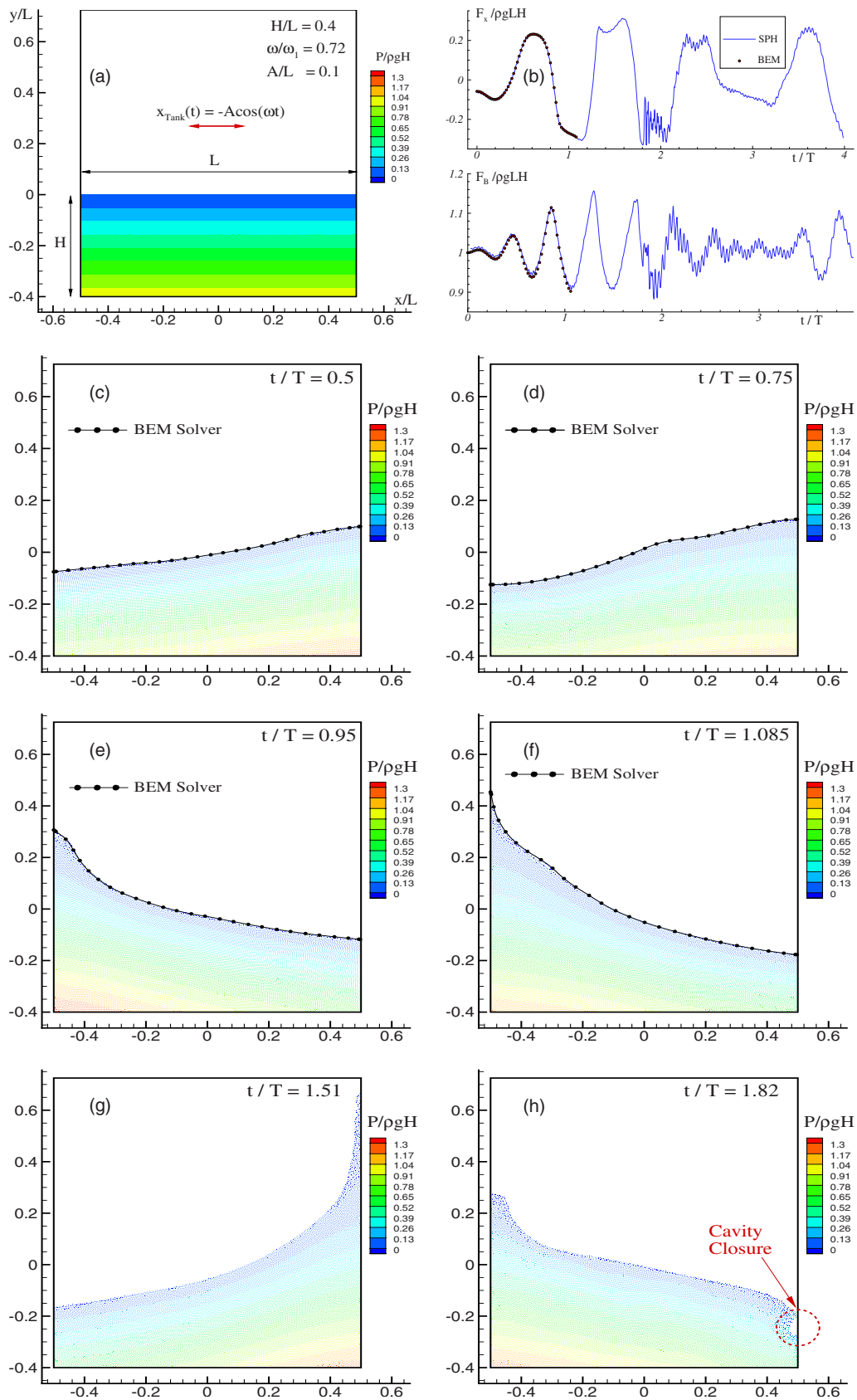
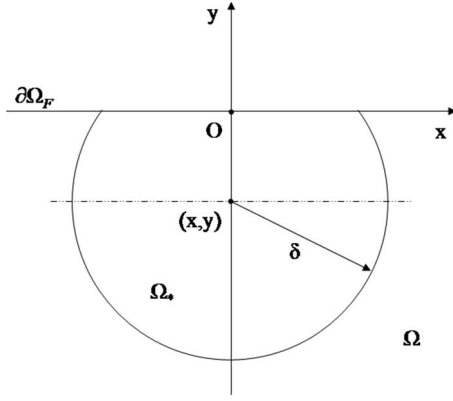


FIG. 4. (Color online) Top-left quadrant: sketch of the sloshing problem. L is the tank width, H is the tank height, A represents the amplitude of the forcing sway motion, ω is its frequency, and ω_1 is the linear first resonant frequency. Top-right quadrant: comparison between the vertical (F_B) and horizontal (F_x) loads as predicted by the SPH solver and by the BEM. Middle and bottom quadrants: snapshots of the fluid motion inside the tank ($T=2\pi/\omega$). The black dotted lines represent the free-surface position evaluated through the BEM.


 FIG. 5. Sketch of the support of W near a flat free surface.

Load” project, and partially done within the framework of the “Programma Ricerche INSEAN 2007–2009” and “Programma di Ricerca sulla Sicurezza” funded by Ministero Infrastrutture e Trasporti.

APPENDIX A: CONVERGENCE OF THE SMOOTHED OPERATOR ($\text{div } \mathbf{u}$) NEAR THE FREE SURFACE

When one wants to study the convergence with h of any smoothed operator close to the free surface, two situations have to be considered: either the point of interest \mathbf{x} is on the free surface $\partial\Omega_F$ or \mathbf{x} is at a distance ϵ of this surface. In the latter case, it always exists that an $h_\epsilon < \epsilon$ such that the support of the kernel is entirely included in the domain Ω .

Mathematically, only the situation where $\mathbf{x} \in \partial\Omega_F$ is thus to be considered. Note that in a practical implementation h has a fixed value, so that there is always an area close to the free surface where the points are influenced by the free-surface presence.

The divergence of \mathbf{u} given by formula (23) represents a special case among the other smoothed quantities. In fact, even if $\mathbf{x} \in \partial\Omega_F$, the volume and the surface integral separately converge to zero as $h \rightarrow 0$. Let us consider the volume integral

$$\int_{\Omega_\star} (\mathbf{u}^\star - \mathbf{u}) \cdot \nabla W(\mathbf{x} - \mathbf{x}^\star) dV^\star = \int_{\Omega_\star} (u_i^\star - u_i) \frac{\partial W(\mathbf{x} - \mathbf{x}^\star)}{\partial x_i} dV^\star, \quad (\text{A1})$$

where the summation for the repeated subindexes is understood. Since we have

$$u_i^\star - u_i = u_i(\mathbf{x}^\star) - u_i(\mathbf{x}) = \frac{\partial u_i(\mathbf{x})}{\partial x_j} (x_j^\star - x_j) + O(\|\mathbf{x}^\star - \mathbf{x}\|^2), \quad (\text{A2})$$

we get

$$\begin{aligned} \int_{\Omega_\star} (\mathbf{u}^\star - \mathbf{u}) \cdot \nabla W(\mathbf{x} - \mathbf{x}^\star) dV^\star \\ = \frac{\partial u_i(\mathbf{x})}{\partial x_j} \int_{\Omega_\star} (x_j^\star - x_j) \frac{\partial W(\mathbf{x} - \mathbf{x}^\star)}{\partial x_i} dV^\star + O(h). \end{aligned} \quad (\text{A3})$$

Let us focus on the last integral of the previous equation and assume $\mathbf{x} \in \partial\Omega_F$. If $\partial\Omega_F$ is a regular curve, for h going to zero it is possible to approximate the free surface by its tangent in \mathbf{x} (see Fig. 5). Then, we have

$$\int_{\Omega_\star} (x_j^\star - x_j) \frac{\partial W(\mathbf{x} - \mathbf{x}^\star)}{\partial x_i} dV^\star = \frac{\delta_{ij}}{2}, \quad (\text{A4})$$

where δ_{ij} is the Kronecker tensor. Then, substituting the previous result in Eq. (A3), we get

$$\begin{aligned} \int_{\Omega_\star} (\mathbf{u}^\star - \mathbf{u}) \cdot \nabla W(\mathbf{x} - \mathbf{x}^\star) dV^\star = \frac{1}{2} \frac{\partial u_i(\mathbf{x})}{\partial x_i} + O(h) = \frac{1}{2} \text{div } \mathbf{u}(\mathbf{x}) \\ + O(h). \end{aligned} \quad (\text{A5})$$

This result is very important since it shows that the convergence rate of the volume integral of $\text{div } \mathbf{u}$ is asymptotically equal to the convergence rate of the initial formula (9) [see (13)]. Finally, since $\text{div } \mathbf{u} = 0$ for $\mathbf{x} \in \partial\Omega_F$, it follows:

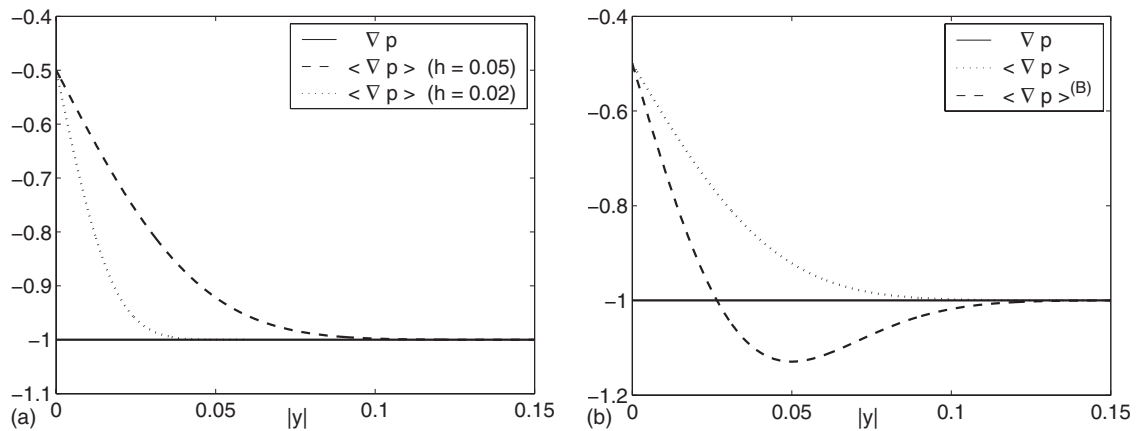


FIG. 6. Left panel: comparison between the analytical pressure gradient (solid line) and $\langle \nabla p \rangle$ (dashed line, $h=0.05$; dotted line, $h=0.02$) for $c_0=1$. Right panel: comparison between the analytical pressure gradient (solid line), $\langle \nabla p \rangle^B$ (dashed line), and $\langle \nabla p \rangle$ (dotted line) for $c_0=1$ and $h=0.05$.

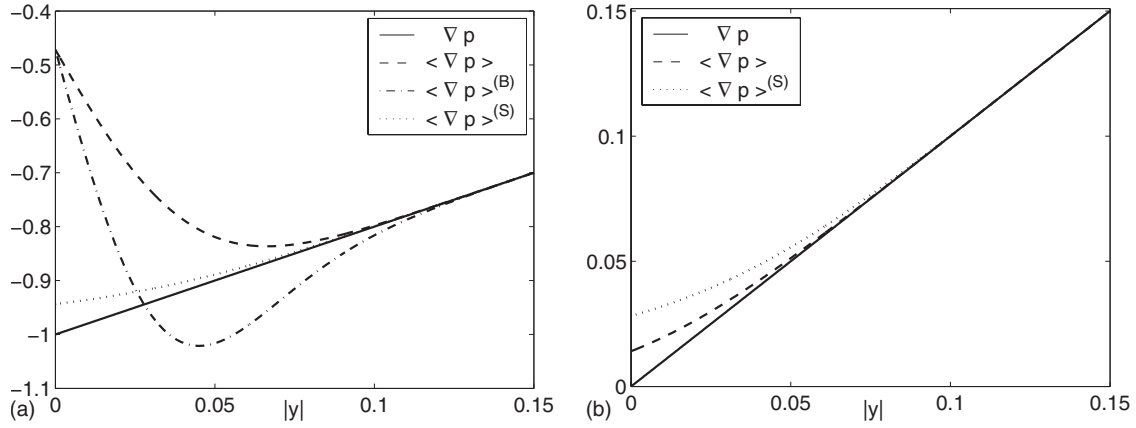


FIG. 7. Left panel: the y derivative of p . Comparison between the analytic solution (solid line), the standard formula (dashed line), the Bonet pressure gradient (dash-dotted line), and the Shepard pressure gradient (dotted line) for the quadratic pressure field ($h=0.05$). Right panel: the x derivative of p . Comparison between the analytic solution (solid line), the standard formula (dashed line), and the Shepard pressure gradient (dotted line) for the quadratic pressure field ($h=0.05$).

$$\int_{\Omega_*} (\mathbf{u}^* - \mathbf{u}) \cdot \nabla W(\mathbf{x} - \mathbf{x}^*) dV^* = O(h). \quad (\text{A6})$$

Applying the same procedure to the surface integral, we get

$$\int_{\partial\Omega_*} (\mathbf{u}^* - \mathbf{u}) \cdot \mathbf{n}^* W dS^* = \frac{\partial u_i(\mathbf{x})}{\partial x_j} \int_{\partial\Omega_*} (x_j^* - x_j) n_i^* W dS^* + O(h). \quad (\text{A7})$$

Since $\mathbf{x}^*, \mathbf{x} \in \partial\Omega_F$, it is $x_2^* = y^* = 0$, $x_2 = y = 0$, $x_1 = x = 0$, and $\mathbf{n} = (0, 1)$ (see Fig. 5). Then, it follows:

$$\int_{\partial\Omega_*} (x_j^* - x_j) n_i^* W dS^* = \int_{-\delta}^{\delta} x^* W dx^* = 0, \quad (\text{A8})$$

since W is a pair function. Finally, we obtain

$$\int_{\partial\Omega_*} (\mathbf{u}^* - \mathbf{u}) \cdot \mathbf{n}^* W dS^* = O(h). \quad (\text{A9})$$

Notwithstanding the latter result, the surface terms play a relevant role in the evaluation of $\langle \text{div } \mathbf{u} \rangle$. In the following paragraph, we show some test cases to highlight such behavior.

APPENDIX B: EXAMPLES OF CONVERGENCE OF THE SMOOTHED OPERATORS USING A GAUSSIAN KERNEL

In order to show some examples of convergence of the smoothed formulas for the two operators $\text{div } \mathbf{u}$ and ∇p , we consider the following renormalized Gaussian kernel:

$$W(\mathbf{x} - \mathbf{x}^*) = \frac{\exp(-\|\mathbf{x} - \mathbf{x}^*\|^2/h^2) - \exp(-\delta^2/h^2)}{\pi h^2 [1 - (1 + \delta^2/h^2)\exp(-\delta^2/h^2)]}, \quad (\text{B1})$$

whose compact support is $B_\delta(\mathbf{x})$ (i.e., the ball centered in \mathbf{x} with radius δ). In the following, we assume $\delta = bh$ where $b = O(1)$. Note that the previous assumption implies that the radius of the support of W vanishes as h goes to zero.

Regarding the geometry of all the following examples, we refer to Fig. 5 where the free surface is at $y=0$ and all the SPH formulas are evaluated along the half axis $y \leq 0$ [that is, the SPH formulas are centered in $\mathbf{x} = (0, y)$ with $y \leq 0$]. Since we are interested in the behavior of the SPH interpolation near the free surface, we also assume $|\mathbf{x}| \leq \delta$, that is, $|y| \leq \delta$. As a consequence, in Figs. 6–11 which follow, we use the distance from the free surface $|y|$ as abscissa.

1. Pressure gradient

We first focus on the pressure gradient. In analogy with the hydrostatic pressure field, we first assume $p = -c_0 y$, where c_0 is a constant (note that $p=0$ along the free surface). The pressure gradient in the x direction is always identically zero and, therefore, we only consider the pressure gradient in the y direction. The left panel of Fig. 6 shows the comparison between the analytical pressure gradient (solid line) and $\langle \nabla p \rangle$ (dashed line) for $c_0=1$ and for different values of h . It is evident that the pressure gradient evaluated through the stan-

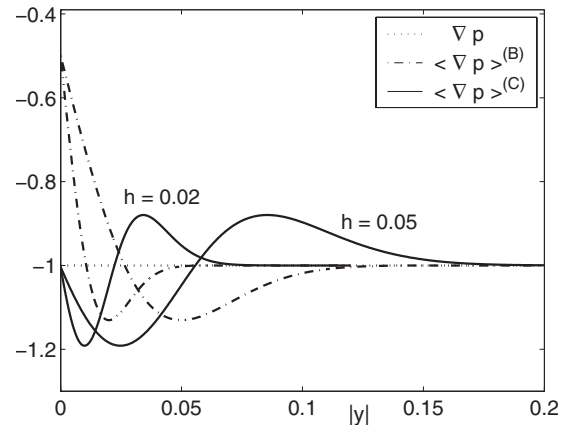


FIG. 8. Comparison between the analytic solution (dotted line), the Bonet pressure gradient (dashed line), and the symmetrized Shepard pressure gradient (solid line) for the linear pressure field ($h=0.05$ and $h=0.02$).

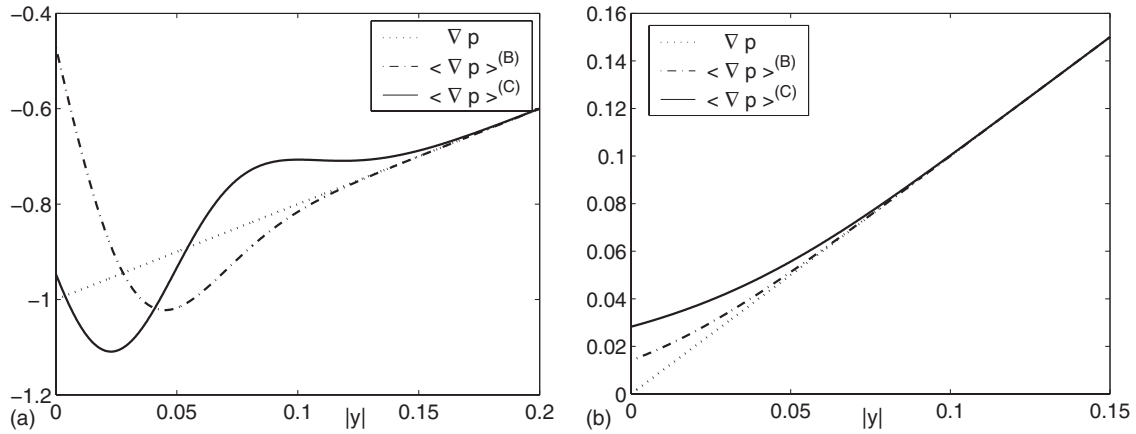


FIG. 9. Comparison between the analytic solution (dotted line), the Bonet pressure gradient (dashed line), and the symmetrized Shepard pressure gradient (solid line) for the quadratic pressure field ($h=0.05$). Left panel: the y derivative of p . Right panel: the x derivative of p .

standard SPH formula halves at $y=0$, even if for $h \rightarrow 0$ the error between ∇p and $\langle \nabla p \rangle$ is limited to the free surface. Similarly, in the right panel of Fig. 6 we show the comparison between the analytical pressure gradient (solid line), $\langle \nabla p \rangle^B$ (dashed line), and $\langle \nabla p \rangle$ (dotted line). One can observe that $\langle \nabla p \rangle^B$ presents a different behavior, oscillating around the analytical solution (the mean error is close to zero). Finally, we note that the Shepard pressure gradient coincides with the analytical one and, therefore, it is not shown.

To round the analysis, we consider a more general case, that is, $p = -c_0 y(1 + c_1 x + c_2 y)$. The pressure field is still zero at $y=0$ but now it also depends on x and, therefore, the x derivative is not identically zero. In the specific, we choose $c_0 = c_1 = c_2 = 1$. The y derivatives evaluated through $\langle \nabla p \rangle$ and $\langle \nabla p \rangle^B$ show a behavior similar to the one described in the hydrostatic case. Conversely, the Shepard pressure gradient is now sensibly different from zero even if it is still the best interpolation (see the left panel of Fig. 7). This is not the case when we focus on the x derivative. In fact, the Shepard pressure gradient gives a result worse than the standard formula (see the right panel of Fig. 7). This is due to the fact that $\partial p / \partial x$ is zero at the free surface and, consequently, the Shepard renormalization gives no advantage in the evaluation of the pressure gradient. Conversely, the Bonet formula coincides with the standard pressure gradient (and, therefore, it is not shown in the figure).

As a final example, we show the comparison between $\langle \nabla p \rangle^C$ and $\langle \nabla p \rangle^B$ for both linear and quadratic pressure fields (Figs. 8 and 9). In both cases, the symmetrized Shepard kernel $\langle \nabla p \rangle^C$ clearly shows a better match with the analytical solutions than $\langle \nabla p \rangle^B$.

2. Velocity divergence

For what concerns the divergence of \mathbf{u} , we first consider a linear velocity field $\mathbf{u} = (x, -y)$ whose divergence is zero everywhere. The left panel of Fig. 10 clearly shows that $\langle \text{div } \mathbf{u} \rangle$ [formula (23)] coincides with $\text{div } \mathbf{u}$. Conversely, the SPH divergence of \mathbf{u} evaluated without the surface terms is quite different from the analytical solution. Moreover, it is also evident that the maximum value of the discrepancy is quite large and does not decrease as h goes to zero. This result is very important since among the SPH practitioners, it is a common practice to neglect the surface terms inside the divergence of \mathbf{u} . The right panel of Fig. 10 shows a sketch of the linear velocity field near the free surface ($y=0$).

Finally, let us consider a purely quadratic field $\mathbf{u} = (x^2 + xy + y^2, x^2 - 2xy + y^2)$, whose divergence is null on $y=0$. In

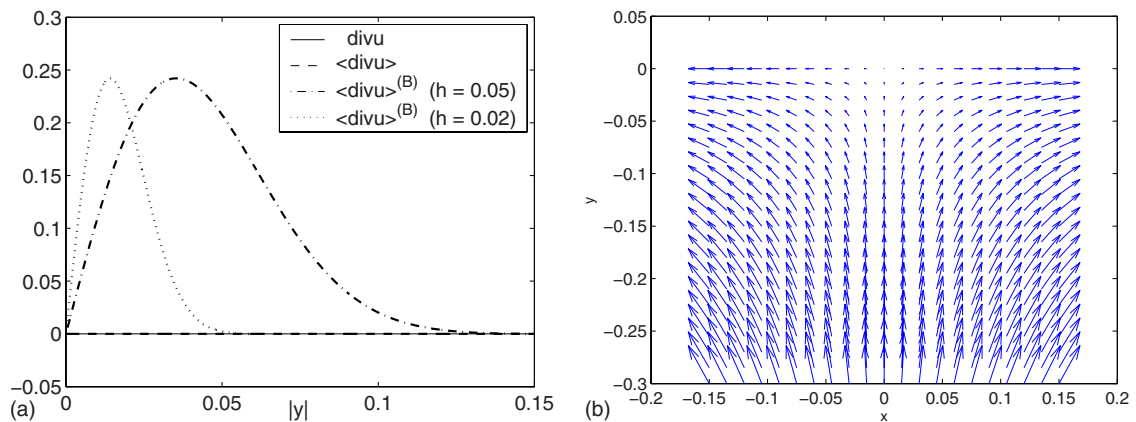


FIG. 10. (Color online) Left panel: comparison between $\text{div } \mathbf{u}$ (solid line), $\langle \text{div } \mathbf{u} \rangle$ (dashed line), and $\langle \text{div } \mathbf{u} \rangle$ without the surface terms (dash-dotted line, $h=0.05$; dotted line, $h=0.02$) for the linear velocity field. Right panel: sketch of the linear velocity field.

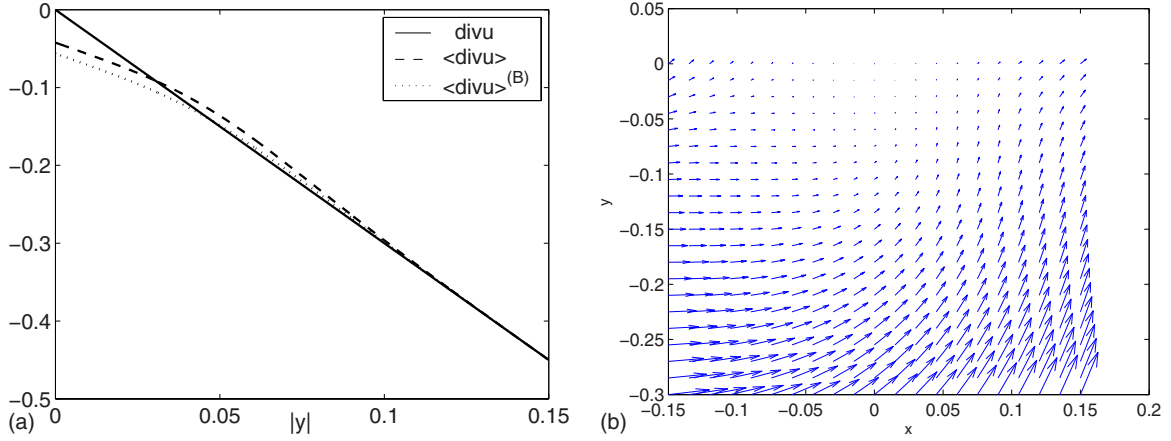


FIG. 11. (Color online) Left panel: comparison between $\text{div } \mathbf{u}$ (solid line), $\langle \text{div } \mathbf{u} \rangle$ (dashed line), and $\langle \text{div } \mathbf{u} \rangle$ without the surface terms (dotted line) for the quadratic velocity field ($h=0.05$). Right panel: sketch of the quadratic velocity field.

this case, the weight of the surface terms is smaller and both $\langle \text{div } \mathbf{u} \rangle$ and its approximation without the surface terms are quite similar to the analytical solution (see left panel of Fig. 11). The right panel of Fig. 11 shows a sketch of the quadratic velocity field close to the free surface ($y=0$).

APPENDIX C: DETAIL OF COMPUTATION FOR THE PVW

We focus on the term ③ in Eq. (25) and we change $\text{div}(\delta \mathbf{w})$ with $\langle \text{div}(\delta \mathbf{w}) \rangle$ [see formula (23)]. We get

$$\begin{aligned}
 \int_{\Omega} p \langle \text{div}(\delta \mathbf{w}) \rangle dV &= \int_{\Omega} p \left[\int_{\Omega} (\delta \mathbf{w}^* - \delta \mathbf{w}) \cdot \nabla W dV^* \right. \\
 &\quad \left. + \int_{\partial \Omega} (\delta \mathbf{w}^* - \delta \mathbf{w}) \cdot \mathbf{n}^* W dS^* \right] dV \\
 &= \int_{\Omega} p \int_{\Omega} \delta \mathbf{w}^* \cdot \nabla W dV^* dV \\
 &\quad - \int_{\Omega} p \delta \mathbf{w} \cdot \int_{\Omega} \nabla W dV^* dV \\
 &\quad + \int_{\Omega} p \int_{\partial \Omega} \delta \mathbf{w}^* \cdot \mathbf{n}^* W dS^* dV \\
 &\quad - \int_{\Omega} p \delta \mathbf{w} \cdot \int_{\partial \Omega} \mathbf{n}^* W dS^* dV. \quad (C1)
 \end{aligned}$$

Now, changing the order of the integrals, we can write

$$\begin{aligned}
 &= \int_{\Omega} \delta \mathbf{w}^* \cdot \int_{\Omega} p \nabla W dV dV^* - \int_{\Omega} p^* \delta \mathbf{w}^* \cdot \int_{\Omega} \nabla^* W dV dV^* \\
 &\quad + \int_{\partial \Omega} \delta \mathbf{w}^* \cdot \mathbf{n}^* \int_{\Omega} p W dV dS^* - \int_{\Omega} p^* \delta \mathbf{w}^* \cdot \int_{\partial \Omega} \mathbf{n} W^* dS dV^*. \quad (C2)
 \end{aligned}$$

Since $W^* = W$ and $\nabla^* W = -\nabla W$, it comes

$$\begin{aligned}
 &= \int_{\Omega} \delta \mathbf{w}^* \cdot \int_{\Omega} p \nabla W dV dV^* + \int_{\Omega} p^* \delta \mathbf{w}^* \cdot \int_{\Omega} \nabla W dV dV^* \\
 &\quad + \int_{\partial \Omega} \delta \mathbf{w}^* \cdot \mathbf{n}^* \langle p \rangle^* dS^* - \int_{\Omega} p^* \delta \mathbf{w}^* \cdot \int_{\partial \Omega} \mathbf{n} W dS dV^*. \quad (C3)
 \end{aligned}$$

One can note that

$$\int_{\partial \Omega} \mathbf{n} W dS = \int_{\Omega} \nabla W dV, \quad (C4)$$

so that it becomes

$$= \int_{\Omega} \delta \mathbf{w}^* \cdot \int_{\Omega} p \nabla W dV dV^* + \int_{\partial \Omega} \delta \mathbf{w}^* \cdot \mathbf{n}^* \langle p \rangle^* dS^* \quad (C5)$$

and from Eq. (15) we have

$$\langle \nabla p \rangle = \int_{\Omega} p^* \nabla W dV^* + \int_{\partial \Omega} p^* \mathbf{n}^* dS^*, \quad (C6)$$

where the last term is zero due to the DFSBC. Finally, one gets

$$\int_{\Omega} p \langle \text{div}(\delta \mathbf{w}) \rangle dV = - \int_{\Omega} \delta \mathbf{w} \cdot \langle \nabla p \rangle dV + \int_{\partial \Omega} \delta \mathbf{w} \cdot \mathbf{n} \langle p \rangle dS, \quad (C7)$$

which is the smoothed version of the PVW.

- [1] L. B. Lucy, *Astron. J.* **82**, 1013 (1977).
- [2] R. A. Gingold and J. J. Monaghan, *Mon. Not. R. Astron. Soc.* **181**, 375 (1977).
- [3] M. Landrini, A. Colagrossi, M. Greco, and M. P. Tulin, *J. Fluid Mech.* **591**, 183 (2007).
- [4] J. Bonet and T. S. L. Lok, *Comput. Methods Appl. Mech. Eng.* **180**, 97 (1999).
- [5] A. Colagrossi and M. Landrini, *J. Comput. Phys.* **191**, 448 (2003).
- [6] S. Mas-Gallic and P. A. Raviart, *Numer. Math.* **51**, 323 (1987).
- [7] A. Colagrossi, Ph.D. thesis, University of Rome La Sapienza, Italy, 2005.
- [8] D. J. Price, *J. Comput. Phys.* **227**, 10040 (2008).
- [9] J. J. Monaghan, *Rep. Prog. Phys.* **68**, 1703 (2005).
- [10] *Mathematical Foundations of Elasticity*, edited by J. E. Marsden and T. J. R. Hughes (Dover, New York, 1994).
- [11] R. Glowinski and P. Le Tallec, *Augmented Lagrangian and Operator-Splitting Methods in Nonlinear Mechanics* (SIAM, Philadelphia, 1989).
- [12] D. Shepard, *A Two-Dimensional Interpolation Function for Irregular Spaced Data*, Proceedings of the 1968 23rd ACM National Conference (ACM, New York, 1968), p. 517.
- [13] G. Colicchio and M. Landrini, *J. Eng. Math.* **46**, 127 (2003).